

# Successive network reduction method for parametric transient results

Márton Németh and András Poppe

Budapest University of Technology and Economics, Department of Electron Devices  
Magyar tudósok krt. 2, Bld. Q, 3rd floor, Budapest, Hungary H-1117, Tel.: +36-1-463-3073

**Abstract**—In this paper we present a new, direct computational method for calculating the complex thermal transfer impedances between two separate locations of a given physical structure aimed at the implementation into a field-solver based on the SUNRED (SUccessive Node REDuction) algorithm. We tested the method with a simple 2D example containing 125 internal nodes. For testing the proposed new calculation method multiple combinations of Dirichlet and Neumann type boundary conditions were applied. Also, different types of thermal loads such as prescribed unit-step change in dissipation or temperature were assumed (for time domain transient analysis). The test case was also studied with the assumption of sinusoidal dissipation. Results obtained by the proposed new calculation method and results obtained by conventional simulations differ less than the uncertainty of the traditional solution method. The good agreement enables us to use the balanced truncation method to reduce the order of the transfer functions with low computational cost.

**Index Terms**—compact thermal modeling, thermal transfer functions, node reduction

|               | Nomenclature                             |
|---------------|--|
| $A$           | Surface area $i$ [ $m^2$ ]               |
| $c_V$         | Volumetric specific heat [ $J/m^3 K$ ]   |
| $C$           | Specific heat for a cell [ $J/K$ ]       |
| $\varepsilon$ | Resolution of the model [ $m$ ]          |
| $G_{Th}$      | Thermal conductance [ $W/K$ ]            |
| $I_{Th}, P$   | Nodal heat flow [ $W$ ]                  |
| $\lambda$     | Thermal conductivity [ $W/m \cdot K$ ]   |
| $\dot{q}'$    | Heat generation rate [ $W/m^3$ ]         |
| $\rho$        | Density [ $kg/m^3$ ]                     |
| $T$           | Temperature or nodal temperature [ $K$ ] |
| $t$           | Time [ $s$ ]                             |
| $dt$          | Time-step [ $s$ ]                        |
| $Y$           | Admittance matrix                        |

## I. INTRODUCTION

We face a growing interest in more accurate thermal modeling of electronic parts, such as ICs, discrete power semiconductor devices and Light-Emitting Diode (LED) devices. In the past two decades the need for higher speed of numerical simulations and the fact that semiconductor vendors do not want to share proprietary information about their advanced packaging solution resulted in the development of compact thermal models of the packages of electronic components. In his 2008 paper [1] C. Lasance provided an overview of the state of the art. From the known methods of that time the DELPHI model topology and modeling methodology became even an industry standard [2]. The DELPHI compact

modeling methodology uses a global optimization method to find the network element values of the DELPHI model of an IC package which fit the best the simulation results for a great variate of different thermal boundary conditions. Since then many new compact modeling methods were developed, including the recent results of L. Codecasa et al [3], [4] and other, reduced order modeling based methods. The order reduction process can be based on projection (as described e.g. in [5]), or elimination of nodes – a method also used in field-solvers such as our in-house, proprietary tool SUNRED (see e.g. [6]).

A particularly effective projection based model can be derived with the so-called multi-point moment matching technique, which solves the projection in the complex frequency domain [3]. Despite the effectiveness of the moment matching, the results are influenced by the chosen points to match the moments. Another question is the robustness and stability of the algorithms, however the novel developments solve these problems [7]. The desirable solution in our opinion would be a balanced reduction based algorithm, but the computational cost of such an algorithm is high  $o(n^3)$  against the cost of moment matching algorithm  $o(n) - o(n^2)$ .

The goal of this paper to describe how would the advantages of the SUNRED method can be united with the use of transfer impedances resulting in a new considerably effective method based on balanced reduction. This new method uses the matrix-operations of the SUNRED algorithm and it is applied to an algebraic equation-system obtained by the Laplace-transform of the original discretized system. During the model building the reduction of the order of the transfer impedances is done, therefore the degree of freedom ( $n$ ) can be held low in each step of the reduction.

## II. MODELING

### A. The SUNRED algorithm

The SUNRED algorithm is centered around the **admittance matrix** of the electrical equivalent circuit derived from the spatially discretized form of thermal diffusion equation [6], [8] in 2D:

$$\frac{\lambda}{\varepsilon^2} (T_{i+1,j} + T_{i-1,j} + T_{i,j+1} + T_{i,j-1} - 4T_{i,j}) = P + c_V \frac{T_{i,j}(t) + T_{i,j}(t - dt)}{dt} \quad (1)$$

This algebraic equation system for the time domain propagation can be written as a matrix-equation:

$$\underline{T}(t + dt) = \underline{T}(t) + dt \cdot \underline{YT} \quad (2)$$

The elements of the matrix can be expressed with the help of the *thermal conductance*:

$$G_{Th} = \frac{Q_{through}}{\Delta T} = \frac{\lambda A}{dx} = \lambda dx \quad (3)$$

The admittance matrix can be written as (in 2D):

$$\underline{Y} = \begin{pmatrix} -4G_{Th} & G_{Th} & G_{Th} & G_{Th} & 0 \cdots 0 \\ G_{Th} & -4G_{Th} & G_{Th} & \ddots & \vdots \\ G_{Th} & G_{Th} & -4G_{Th} & \ddots & \vdots \\ \vdots & \ddots & \ddots & \ddots & \vdots \\ G_{Th} & 0 \cdots 0 & G_{Th} & G_{Th} & -4G_{Th} \end{pmatrix} \quad (4)$$

where  $G_{Th}$  appears in the  $i^{th}$  row  $j^{th}$  column, if the node at  $(x, y)$  coordinate, which belongs to the row  $i$  in the matrix, is connected to another node (i.e.  $x, y - 1$ ) which is represented by column  $j$ . The other elements of the matrix are zero indicating the lack of direct connection between the represented nodes. This matrix can be used to determine the heat fluxes between nodes by applying Kirchhoff's laws:

$$\underline{I}_{Th} = \underline{YT} + \underline{I}_{gen} \quad (5)$$

where  $\underline{I}_{Th}$ ,  $\underline{T}$  and  $\underline{I}_{gen}$  are vectors with  $N$  element that represent each node. The steady-state thermal solution can be derived from Eq. (5) with the assumption of  $\underline{I}_{Th} = 0$ :

$$\underline{T} = -\underline{Y}^{-1} \underline{I}_{gen}. \quad (6)$$

The order of the admittance matrix can be reduced by merging the neighboring nodes with the so-called *successive node reduction* (SUNRED) algorithm, which is an algebraic form of the Y- $\Delta$  transformation, and so that can be applied not just for resistive network, but for a network with complex impedances.

To show the steps of the SUNRED algorithm we chose a simple building block with four external and one internal node as in Figure 1. The admittance matrix of such a block can be written as:

$$\underline{Y} = \begin{pmatrix} -G_{Th} & 0 & 0 & 0 & G_{Th} \\ 0 & -G_{Th} & 0 & 0 & G_{Th} \\ 0 & 0 & -G_{Th} & 0 & G_{Th} \\ 0 & 0 & 0 & -G_{Th} & G_{Th} \\ G_{Th} & G_{Th} & G_{Th} & G_{Th} & -4G_{Th} \end{pmatrix} \quad (7)$$

that also represents one of the four building blocks in Figure 2. The rows and columns of 1–4 represent the connections of the nodes on the side of the rectangle, while the fifth row and column represents the central node's connections of a standalone building block. Now we established all the connections for the central node (that won't connect to more nodes), therefore it can be eliminated. The elimination process:

$$\underline{Y}_{red} = \underline{Y}_{out} - \underline{Y}_{in-out} \underline{Y}_{in}^{-1} \underline{Y}_{out-in} \quad (8)$$

where  $\underline{Y}_{red}$  is the reduced admittance matrix,  $\underline{Y}_{out}$  is the matrix of the connections only from the maintained nodes (in the

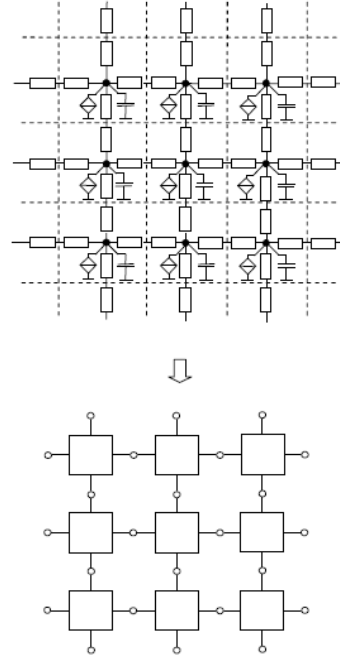


Figure 1: SUNRED algorithm a) 3D rectangular field b) SUNRED version of Finite Differences model in 2D b) The model after the first node reduction step (elimination of the internal nodes of the first level cells) [9]

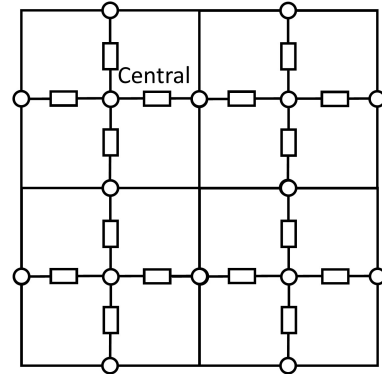


Figure 2: Four two dimensional building blocks in a network

example the rows and columns form 1 to 4),  $\underline{Y}_{in-out}$  contains the connection between the inner and outer nodes (fifth row 1–4 columns), as the  $\underline{Y}_{out-in}$  (fifth column 1–4 rows) and  $\underline{Y}_{in}$  stands for the inner node connections (fifth column and row). Therefore, the reduced matrix of the building block becomes:

$$\underline{Y}_{red} = \frac{G_{Th}}{4} \begin{pmatrix} -3 & 1 & 1 & 1 \\ 1 & -3 & 1 & 1 \\ 1 & 1 & -3 & 1 \\ 1 & 1 & 1 & -3 \end{pmatrix} \quad (9)$$

The connection between the building blocks can be established by merging the common nodes' rows and columns.

In case of transient simulation, the capacitors representing the thermal capacitance of a grid cell are replaced with their time-discretized resistive equivalent corresponding to the

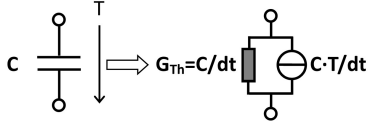


Figure 3: The time discretized resistive equivalent of a capacitor (for the time-domain numerical integration scheme based on the reverse Euler method)

actual time-domain numerical solution method. Basically, such an equivalent represents a capacitor with a resistor and with a "current" source. In case of thermal capacitance the source value is equal to the heat-flux resulting from the change of the thermal energy stored in the volume of material represented by the simulation grid cell during the given simulation time interval  $\Delta t$  simulation time-step (see Figure 3) therefore the whole temperature-map must be recalculated for the subsequent simulation time-steps.

### III. SUNRED ALGORITHM WITH TRANSFER FUNCTIONS REPRESENTING THERMAL TRANSFER IMPEDANCES

With the Laplace transform of Eq.:(1) the SUNRED algorithm can also be formulated for the system behavior in the complex frequency ( $s$ ) domain as follows:

$$\frac{\lambda}{\varepsilon^2} (T_{i+1,j}(s) + T_{i-1,j}(s) + T_{i,j+1}(s) + T_{i,j-1}(s) - 4T_{i,j}(s)) = P + c_V s T_{i,j}(s) \quad (10)$$

This means that the admittance matrix itself depends on the complex frequency  $s$  (in the Laplace domain), therefore the building blocks need to be modified as follows:

$$\underline{\underline{Y}} = \begin{pmatrix} -G_{Th} & 0 & 0 & 0 & G_{Th} \\ 0 & -G_{Th} & 0 & 0 & G_{Th} \\ 0 & 0 & -G_{Th} & 0 & G_{Th} \\ 0 & 0 & 0 & -G_{Th} & G_{Th} \\ G_{Th} & G_{Th} & G_{Th} & G_{Th} & -4G_{Th} - Cs \end{pmatrix} \quad (11)$$

where  $C$  stands for the thermal capacitance of a whole block, as shown in Figure 4. The reduction algorithm is the same as outlined above, therefore the reduced building block can be represented with the following equation:

$$\underline{\underline{Y}}_{red} = \begin{pmatrix} \frac{G_{Th}^2}{4G_{Th} - Cs} - G_{Th} & \frac{G_{Th}^2}{4G_{Th} - Cs} & \frac{G_{Th}^2}{4G_{Th} - Cs} & \frac{G_{Th}^2}{4G_{Th} - Cs} \\ \frac{G_{Th}^2}{4G_{Th} - Cs} & \frac{G_{Th}^2}{4G_{Th} - Cs} - G_{Th} & \frac{G_{Th}^2}{4G_{Th} - Cs} & \frac{G_{Th}^2}{4G_{Th} - Cs} \\ \frac{G_{Th}^2}{4G_{Th} - Cs} & \frac{G_{Th}^2}{4G_{Th} - Cs} & \frac{G_{Th}^2}{4G_{Th} - Cs} - G_{Th} & \frac{G_{Th}^2}{4G_{Th} - Cs} \\ \frac{G_{Th}^2}{4G_{Th} - Cs} & \frac{G_{Th}^2}{4G_{Th} - Cs} & \frac{G_{Th}^2}{4G_{Th} - Cs} & \frac{G_{Th}^2}{4G_{Th} - Cs} - G_{Th} \end{pmatrix} \quad (12)$$

Merging the nodes between blocks and the standard node elimination of the successive node reduction method require the same algebraic operation as in the ordinary SUNRED algorithm [10]. The only difference is that now one has to cope with transfer functions. We can appoint some nodes that will not be eliminated and so we can prescribe the value of the heat flux through such a node or we can prescribe temperature of such nodes. Following the terminology introduced by D. Schweitzer [11], [12]. Let us call such nodes as **driving points** and/or **monitoring points**. When a node is a driving point it

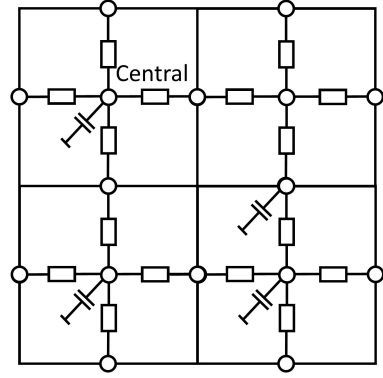


Figure 4: Four two dimensional building blocks with capacitor in a network

represent a time variant heat dissipating element (In a network diagram representing the discretized model such a node is driven by a "current source"). Monitoring points are locations where we would like to know the e.g. the time evolution of the temperature while the state of other such nodes is changing. A node can be both a driving point and a monitoring point. The number of driving points in a system is equal to the number of elementary heat-sources we have in the system. Since any location in the system can be a monitoring point, in a general case the number of monitoring points can be greater or equal to the number of driving points [12]. When the reduction process ends the admittance matrix is an  $n$  times  $n$  matrix of transfer functions. These transfer functions represent the propagation properties between pairs of driving and monitoring points. To extend the terminology to the transfer functions, the node at the "input" side is called driving point (regardless if it is really driven by a heat-source), the node at the "output" side is a monitoring point. Because of the new non-numerical parameter ( $s$ ) in the node reduction process, the thermal resistances and capacitances can also be handled symbolically. In other words, a symbolic transfer function can be created which represents the thermal transfer impedance between two selected nodes of the discretized model of the physical structure (geometry, set of boundary conditions) – changes in materials can be easily applied through changing the resistance and capacitance values accordingly, without the need of performing the time-consuming node reduction algorithm again.

The most significant difference between the original SUNRED algorithm and the proposed algorithm is that the latter is not another reduction method, which makes the simulation faster, but a node-reduction method, which gives the relation between the monitoring and driving points. The transfer function between the nodes gives us all of the possible information at once and it is independent from applied heat on the driving points. As we will show in the next paragraph we can set up parametric material properties, which shows that the given parametric transfer function contains the information from the geometry.

#### IV. PROTOTYPE IMPLEMENTATION AND TESTING

##### A. Simulation setups

The calculation described in the previous subsection was implemented in Matlab 2014 with the help of Matlab's symbolic toolbox. The test setup contained 25 building blocks, and 125 nodes. Homogenous material distribution was assumed in the simulated physical domain. The new transfer impedance calculation method implemented in the SUNRED algorithm was compared with the time-domain thermal transfer impedance functions obtained the standard thermal transient simulation method of the conventional SUNRED solver. In both cases the same geometry and the same sets of boundary conditions were applied. The simulated test structure is shown in Figure 5.

##### B. Results

The model error was investigated by comparing the results on a simple test case (Figure 5) for both a traditional method, and the new method in case of different excitations applied at an arbitrary node of the structure. The applied thermal loads (excitations) were:

- forced step-wise heat-flux,
- forced, step-wise temperature rise,
- forced, time dependent heat-flux (with sinusoidal waveform).

The results obtained by our new calculation method are assumed to theoretically accurate (loaded only with numerical noise due to the finite precision of the representation of floating point numbers) as they are analytically calculated, therefore when we compared them with the results obtained by a conventional SUNRED simulation they were considered as base-line. In case of transient simulation of the conventional SUNRED solver which is based on an Euler-type numerical integration scheme, the inherent numerical error is proportional with the applied  $\Delta t$  simulation time step.

##### C. Error of the Euler method

The difference between the traditional and new method was investigated on the simple geometry described above. After the node reduction process only two monitoring nodes remained which were originally connected to the two transverse corners of the simulated rectangular area (see Figure 5). The boundary condition settings were the following:

- Dirichlet-type conditions with  $0^\circ\text{C}$  applied at the eliminated nodes
- and Neumann-type conditions for the monitoring nodes with  $\pm 1$  W heat flux,

as it is shown in Figure 5 (a). The transient simulation results with different time-steps are shown in Figure 6. The error can be calculated as the average of the absolute value of the relative difference:

$$Error = \sum_{t_i} \frac{T_{new}(t_i) - T_{iter}(t_i)}{T_{new}(t_i)} \quad (13)$$

The results are summarized in Table I. As it is visible the error is linearly decreasing with the size of the  $\Delta t$  time-step – corresponding to our initial assumptions.

In the second test case the same structure was simulated as before, but with 0 W Neumann-type boundary condition as shown in Figure 5. (b). The result are presented in Figure 7. The size of the time-step of the time domain integration of the classical SUNRED solver was  $10^{-7}$  s. In the third example temperature step excitation was applied on one of the free nodes, and the temperature change on the other node as a response was recorded, as illustrated in Figure 5. (c). The obtained results are shown in Figure 8.

In the fourth test case a sinusoidal excitation was applied (see Figure 5 (d)). In (Figure 9), we show the Bode-diagram representation of the transfer impedance, obtained by both methods. We chose a frequency with low attenuation ( $\omega = 100$ ) and a higher frequency for higher attenuation ( $\omega = 10^5$ ). The results are shown in Figure 10 for low frequency and in Figure 11 for high frequency behavior. One can see that on high frequencies the system damping cause an averaging behavior, while in lower frequencies the the transposition is shape-trusty. These results shows that the SUNRED algorithm is adaptable for calculating the complex transfer impedances between far nodes of a grid. We have to note that the new reduction scheme is applied only once for all of the cases above, while the original SUNRED algorithm had to be applied for each case. Calculating the transfer functions lasted for 14 seconds on a 3.2 GHz CPU, while solve one case with the original SUNRED algorithm lasted less than a millisecond. That is a huge difference, but if the ability of parametrization, and the number of runs taken into consideration the new method can be competitive with the original algorithm.

##### D. Order reduction

The most disadvantage of the presented method is the huge runtime. To overcome this problem, we propose to use order reducing algorithm in complex frequency space in each step of building the model. That means the order reduction in each connection step and after each node-reduction step. The algorithm of balanced reduction can be found in the literature [13]. In that way, the balanced reduction is done only on low order systems (less than 20), therefore the computational cost is always low. While the model is being built up, only the

| Time-step (s)     | Error ( $\times 10^{-5}$ ) |
|-------------------|----------------------------|
| $10^{-5}$         | 930                        |
| $5 \cdot 10^{-6}$ | 460                        |
| $2 \cdot 10^{-6}$ | 180                        |
| $10^{-6}$         | 89                         |
| $10^{-7}$         | 7.9                        |
| $10^{-8}$         | 0.9                        |
| $10^{-9}$         | 0.09                       |
| $10^{-10}$        | 0.009                      |

Table I: Effect of the size of time-step on the error

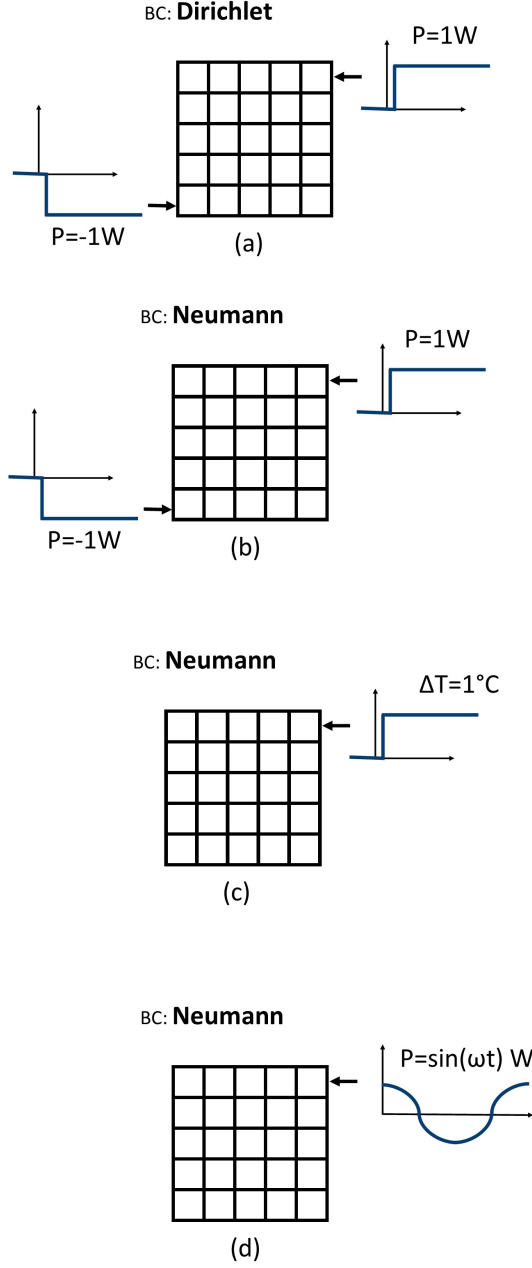


Figure 5: Boundary conditions for different simulations

surficial nodes behave as monitoring nodes, therefore the size of the admittance matrix is proportional to the number of nodes on the surface. In 2D we assume that the computational cost is proportional to  $n^2$ , because the surface is proportional to  $n$ , and the cost of the matrix operations are proportional to  $n^2$ . For the sake of simplicity we examined the former structure of rectangle with more nodes inside. The measured runtimes are summarized in Table II. with the used balanced truncation to 6<sup>th</sup> order of transfer functions. These runtimes are the worst-case results, because of the used square shaped field. The

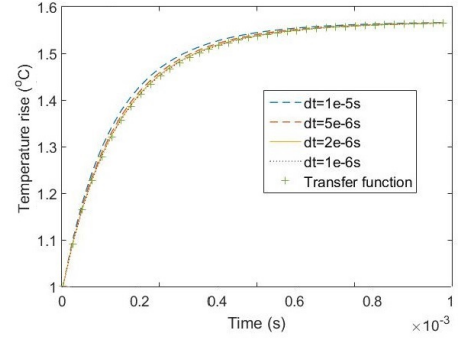


Figure 6: The effect of changing the time-step

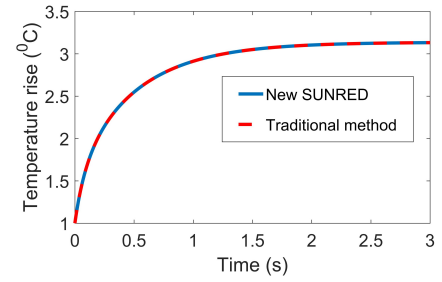


Figure 7: Results for Neumann boundary condition (b)

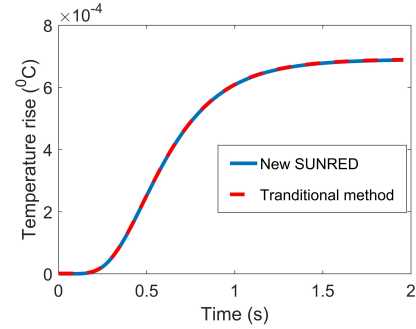


Figure 8: Results for Dirichlet boundary condition (c)

| Number of nodes ( $n$ ) | Runtime (s) |
|-------------------------|-------------|
| 320                     | 1           |
| 1280                    | 1.3         |
| 5120                    | 1.6         |
| 20480                   | 2.1         |
| 81920                   | 3.5         |
| 327680                  | 8.5         |
| 1310720                 | 28          |
| 5242880                 | 103         |
| 20971520                | 258         |

Table II: Runtime versus number of nodes with balanced reduction of 2D square shaped structure

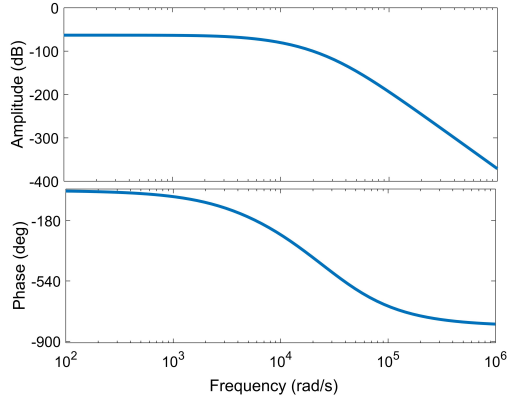


Figure 9: The bode plot of the system (d)

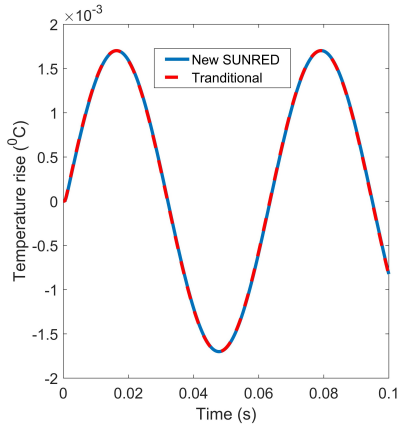


Figure 10: System simulation results for  $\omega = 100$

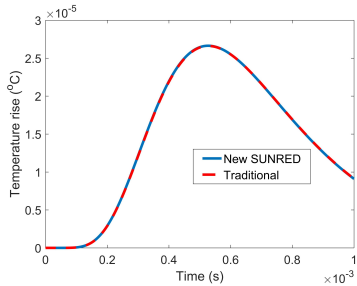


Figure 11: System simulation results for  $\omega = 10^5$

implementation was done by Matlab 2016b, with the help of `balred()` function. The runtimes shows that the computational cost increasing near linearly, which is a consequence of the 2D modeling. That indicates that the new method will be highly effective on flat structures, such as LEDs.

## V. CONCLUSION

We proposed a new modeling method that can be considered as an analytic compact model of thermal transfer impedances. The new modeling method is accurate, parametric and bound-

ary independent. For four different simple test cases the results obtained by the proposed method were compared to the results obtained by a conventional SUNRED algorithm based thermal simulation code. The reduction scheme is naturally time-consuming, in our test case it was 14 seconds, which is at least 1000 times higher than the original SUNRED algorithms runtime. To reduce the runtimes we propose to apply the traditionally time-consuming balanced reduction method with considerably low cost of computation because with the SUNRED method the order of the transfer functions remains low during the reduction process.

## VI. ACKNOWLEDGEMENT

The contribution of the European Union for supporting this study in the context of the H2020 ECSEL Joint Undertaking program (2016-2019) within the frames of the Delphi4LED project (grant agreement 692465) is acknowledged. Co-financing of the Delphi4LED project by the Hungarian government through the NEMZ\_15-1-2016-0033 grant of the National Research, Development and Innovation Fund is also acknowledged.

## REFERENCES

- [1] C. J. M. Lasance, "Ten Years of Boundary-Condition-Independent Compact Thermal Modeling of Electronic Parts: A Review," *Heat Transfer Engineering*, vol. 29, pp. 149–168, feb 2008.
- [2] JEDEC JESD15 Standard, "Methodology for the Thermal Modeling of Component Packages," 2008.
- [3] L. Codecasa, "Nonlinear dynamic compact thermal models by structure-preserving projection," *Microelectronics Journal*, vol. 45, pp. 1764–1769, dec 2014.
- [4] L. Codecasa, A. Magnani, N. Rinaldi, *et al.*, "Structure-preserving approach to multi-port dynamic compact models of nonlinear heat conduction," *Microelectronics Journal*, vol. 46, pp. 1129–1137, dec 2015.
- [5] L. Codecasa, "Compact Models of Dynamic Thermal Networks with Many Heat Sources," *IEEE Transactions on Components and Packaging Technologies*, vol. 30, pp. 653–659, dec 2007.
- [6] Z. Kohári, V. Székely, M. Rencz, A. Páhl, V. Dudek, and B. Höflinger, "Studies on the heat removal features of stacked SOI structures with a dedicated field solver program (SUNRED)," *Microelectronics Reliability*, vol. 38, pp. 1881–1891, dec 1998.
- [7] P. Benner and L. Feng, "A robust algorithm for parametric model order reduction based on implicit moment matching," in *Reduced Order Methods for Modeling and Computational Reduction*, pp. 159–185, Springer International Publishing, 2014.
- [8] A. Páhl, V. Székely, M. Rosenthal, and M. Rencz, "3D extension of the SUNRED field solver," in *1998 4th International Workshop on Thermal Investigations of ICs and Systems (THERMINIC)*, pp. 185–190, 1998.
- [9] L. Pohl, "Multithreading and Strassen's algorithms in SUNRED field solver," in *2008 14th International Workshop on Thermal Investigation of ICs and Systems (THERMINIC)*, sep 2008.
- [10] M. Nemeth, L. Jani, and A. Poppe, "Compact modeling approach for microchannel cooling aimed at high-level thermal analysis of 3D packaged ICs," in *2016 Symposium on Design, Test, Integration and Packaging of MEMS/MOEMS (DTIP)*, may 2016.
- [11] D. Schweitzer, "Generation of multisource dynamic compact thermal models by RC-network optimization," in *29th IEEE Semiconductor Thermal Measurement and Management Symposium (SEMI-THERM)*, mar 2013.
- [12] D. Schweitzer, F. Ender, G. Hantos, and P. G. Szabó, "Thermal transient characterization of semiconductor devices with multiple heat sources—Fundamentals for a new thermal standard," *Microelectronics Journal*, vol. 46, pp. 174–182, feb 2015.
- [13] N. Lang, J. Saak, and T. Stykel, "Balanced truncation model reduction for linear time-varying systems," *Mathematical and Computer Modelling of Dynamical Systems*, vol. 22, pp. 267–281, jun 2016.